Advanced Robotics

ISSN: 0169-1864 (Print) 1568-5535 (Online) Journal homepage: https://www.tandfonline.com/loi/tadr20

A novel method for camera external parameters online calibration using dotted road line

Hai Wang, Yingfeng Cai, Guoyu Lin & Weigong Zhang

To cite this article: Hai Wang, Yingfeng Cai, Guoyu Lin & Weigong Zhang (2014) A novel method for camera external parameters online calibration using dotted road line, Advanced Robotics, 28:15, 1033-1042, DOI: 10.1080/01691864.2014.902329

To link to this article: https://doi.org/10.1080/01691864.2014.902329

Advanced Robotics, 2014
Vol. 28, No. 15, 1033–1042, http://dx.doi.org/10.1080/01691864.2014.902329

Taylor & Francis
Taylor & Francis Group

FULL PAPER

A novel method for camera external parameters online calibration using dotted road line

Hai Wang[a], Yingfeng Cai[a]*, Guoyu Lin[b] and Weigong Zhang[b]

[a]*School of Automotive and Traffic Engineering, Jiangsu University, Zhenjiang, China;* [b]*School of Instrument Science and Engineering, Southeast University, Nanjin, China*

(*Received 7 August 2013; revised 2 January 2014; accepted 15 February 2014*)

On board camera is the most important information source for driver assistant application which is based on computer vision. One problem for on board camera is that the external parameters are easy to be changed when moving on the road. Traditional method either calibrates external parameters offline or calibrates external parameters semi-online, which both need human intervention. By observation, it is found that corner connection of dotted road lane can form two groups of parallel lines. Using this geometric characteristics and through theoretical derivation, a novel online camera external parameter calibration method is proposed which focus on the situation when vehicle is moving. The pro of this method is that it maintains relatively high calculation accuracy and more important, it does not require any human intervention in whole calibration process. Experimental and comparison results show that this method is simple and have accurate results which fully meet the requirements of practical application.

Keywords: online calibration; camera external parameter; dotted road line; advanced driver assistant

1. Introduction

Cameras have been more and more used in vehicles in many fields such as road environment perception for autonomous navigation.[1–6] To make a better use of cameras, the parameters of these on board cameras need to be calibrated accurately. Camera parameters maintain two parts, internal parameters and external parameters. The internal parameters are easy to obtain in a laboratory environment and will not easily change when in use. While the external parameters just can be calibrated after the cameras have been installed in the vehicle. Besides, the external parameters may have a high probability to be changed when driving, because of vehicle vibration or payload variety.

At present, researchers all over the world have conducted extensive research on the external parameters calibration for onboard cameras. In papers [7] and [8], Miyagawa and Jing both use pre-placement mark to calibrate when the vehicle is on a stationary state. These calibration method is accurate but cannot solve the issue of camera parameters changing when vehicle is moving. Michael Miksch and Bin Yang proposed an automatic extrinsic camera self-calibration method based on homography and epipolar geometry.[9] However, they need two cameras to implement this calibration. Meng and Xiangjing present an extrinsic calibration method based on a parametrically described lane marking in the vehicle coordinate system using an Extended Kalman Filter.[10] Qing proposed an online calibration algorithm using road line but they need to know the position of the vehicle relative to the line in advance which is difficult to obtain while vehicle is moving.[11] Yu require making certain rotation angle of the camera to zero to carry out online calibration, but this method requires a certain degree of human intervention, which greatly increases the complexity of the calibration and cannot be used in unmanned vehicles.[12] So that designing of a low human intervention online external parameter calibration method is critical.

In this paper, the geometric characteristics of dotted road line in standard road are analyzed. By analysis, it is found that edge points of dotted road line can form two groups of parallel lines in world coordinate. Using this important geometrical feature, through theoretical derivation, an online camera external parameter calibration method is proposed which is still effective when the vehicle is moving. Our main contribution is that this online method can be used without any adjustment of camera or the vehicle position and no human intervention is needed in the whole calibration process.

2. Camera model

By using traditional pinhole model, camera model is easy to be established like below.

*Corresponding author. Email: yfcai@mail.ujs.edu.cn

$$
\begin{aligned}
Z_c\begin{bmatrix} u \\ v \\ 1 \end{bmatrix} &= \boldsymbol{N}_1 \cdot \boldsymbol{N}_2 \cdot \boldsymbol{N}_3 \begin{bmatrix} X_w \\ Y_w \\ Z_w \\ 1 \end{bmatrix} \\
&= \begin{bmatrix} 1/d_x & 0 & u_0 \\ 0 & 1/d_y & v_0 \\ 0 & 0 & 1 \end{bmatrix} \begin{bmatrix} f & 0 & 0 & 0 \\ 0 & f & 0 & 0 \\ 0 & 0 & 1 & 0 \end{bmatrix} \begin{bmatrix} \boldsymbol{R} & \boldsymbol{t} \\ 0^T & 1 \end{bmatrix} \begin{bmatrix} X_w \\ Y_w \\ Z_w \\ 1 \end{bmatrix} \\
&= \begin{bmatrix} \alpha_x & 0 & u_0 \\ 0 & \alpha_y & v_0 \\ 0 & 0 & 1 \end{bmatrix} [\boldsymbol{R} \quad \boldsymbol{t}] \begin{bmatrix} X_w \\ Y_w \\ Z_w \\ 1 \end{bmatrix} = \boldsymbol{A}[\boldsymbol{R} \quad \boldsymbol{t}] \begin{bmatrix} X_w \\ Y_w \\ Z_w \\ 1 \end{bmatrix} \\
&= \boldsymbol{N} \begin{bmatrix} X_w \\ Y_w \\ Z_w \\ 1 \end{bmatrix}
\end{aligned} \tag{1}
$$

In which, $\alpha_x = f/d_x$, $\alpha_y = f/d_y$.

In Equation (1), α_x, α_y, u_0, v_0 are called camera's internal parameters which are relative to the internal structure of the camera. Matrix $\boldsymbol{A}$ is called the internal parameter matrix. $X_w, Y_w, Z_w, \varphi, \theta, \psi$ are called camera's external parameters because they are decided by the relationship of camera coordinate and world coordinate. Matrix $[\boldsymbol{R} \quad \boldsymbol{t}]$ is called external parameter matrix. The internal parameters are relatively stable when moving, so an offline calibration is acted firstly in the laboratory to maintain the internal parameter matrix. Till now, the work is focused on calibrating the external parameters which will be proposed in the next chapter in detail.

3. Online calibration of external parameters

3.1. Establishment of camera coordinate and world coordinate

First, world coordinate system needs to be built. World coordinate system Σ_w is partially associated on the camera and partially associated with road forward direction.

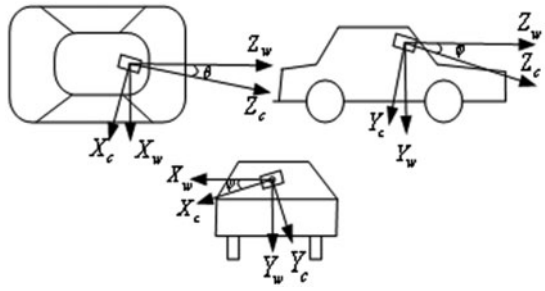

Figure 1. Definition of coordinate system.

The origin O_w of the world coordinate system Σ_w is set on the ground plane under the center of camera coordinate O_C. Axis Z_w is parallel to the road lane. Y_w is perpendicular to the ground plane and point to the upper side of the road. X_w, Y_w, Z_w obey Right-hand screw rule.

Then, camera coordinate system Σ_c is built. The origin of camera coordinate system is in the Y_w axis. X_c, Y_c, Z_c means the three axis of camera coordinate system. It is assumed that the orientation of camera coordinate system is same of the world coordinate system. After that the attitude of Σ_c is expressed by three YXZ Euler angles: θ (rotation angle around the original Y_c axis); and φ (rotation angle around the new X_c axis); ψ (rotation angle around the new Z_c axis). These two coordinates are showed in Figure 1.

Till now, it is clear that the calibration work is to get the value of three rotation angles θ, φ, ψ and the offsets h of camera coordinate system origin in the world coordinate system. In reality, h can be considered as the camera mounting height in the car and will not change when moving. So h can be obtained by previous measurement.

The rotation matrix between camera coordinate system and the world coordinate system using YXZ Euler angle is listed in Equation (2).

$$
\begin{aligned}
\boldsymbol{R} &= \begin{bmatrix} \cos\theta & 0 & \sin\theta \\ 0 & 1 & 0 \\ -\sin\theta & 0 & \cos\theta \end{bmatrix} \begin{bmatrix} 1 & 0 & 0 \\ 0 & \cos\varphi & -\sin\varphi \\ 0 & \sin\varphi & \cos\varphi \end{bmatrix} \begin{bmatrix} \cos\psi & -\sin\psi & 0 \\ \sin\psi & \cos\psi & 0 \\ 0 & 0 & 1 \end{bmatrix} \\
&= \begin{bmatrix} \cos\theta\cos\psi + \sin\theta\sin\varphi\sin\psi & -\cos\theta\sin\psi + \sin\theta\sin\varphi\cos\psi & \sin\theta\cos\varphi \\ \cos\varphi\sin\psi & \cos\varphi\cos\psi & -\sin\varphi \\ -\sin\theta\cos\varphi + \cos\theta\sin\varphi\sin\psi & \sin\theta\sin\psi + \cos\theta\sin\varphi\cos\psi & \cos\theta\cos\varphi \end{bmatrix} \\
&= \begin{bmatrix} r_{11} & r_{12} & r_{13} \\ r_{21} & r_{22} & r_{23} \\ r_{31} & r_{32} & r_{33} \end{bmatrix}
\end{aligned} \tag{2}
$$

So that the external parameter matrix of the two systems is showed in Equation (3):

$$[\boldsymbol{R}\ \boldsymbol{t}] = \begin{bmatrix} r_{11} & r_{12} & r_{13} & 0 \\ r_{21} & r_{22} & r_{23} & -h \\ r_{31} & r_{32} & r_{33} & 0 \end{bmatrix} \tag{3}$$

3.2. *Calibration of camera's external parameters*

In Section 3.1, the relationship between camera coordinate and world coordinate has been built. This section will propose the calibration method in detail. Here, it is assumed that:

(1) The road surface is in the same plane.
(2) The road has two parallel dotted road lines.

Using Equations (1)–(3), the relationship between pixel plane coordinate system points and the world coordinate system points can be written in Equation (4):

$$\begin{cases} Z_c = r_{31}X_w + r_{32}Y_w + r_{33}Z_w \\ u = \dfrac{X_w(\alpha_x r_{11} + u_0 r_{31}) + Y_w(\alpha_x r_{12} + u_0 r_{32}) + Z_w(\alpha_x r_{13} + u_0 r_{33})}{Z_c} \\ v = \dfrac{X_w(\alpha_y r_{21} + v_0 r_{31}) + Y_w(\alpha_y r_{22} + v_0 r_{32}) + Z_w(\alpha_y r_{23} + v_0 r_{33}) - h\alpha_y}{Z_c} \end{cases} \tag{4}$$

Then the calibration method is proposed in three steps:

(a) *Edge points detection in straight line*
Using edge detection method proposed in [13], all the inner side edge feature points of the road lane are detected. Then using these detected inner side edge points, a hyperbola curve is fitted. If the hyperbola coefficient k is small than 50, the road line can be considered as a straight line and go to step (b). Otherwise, process step (a) again.
The hyperbola function is:

$$u = \frac{k}{v - h} + b(v - h) + c \tag{5}$$

(b) *Establishment of double parallel line groups*
Using Harris corner detection algorithm, so that, all the corners in these two inner side straight lines are detected. During the corner points that are found, pick four corner points p_A, p_B, p_C, p_D so that their corresponding points in world coordinate system P_A, P_B, P_C, P_D satisfy $\overline{P_AP_B} = \overline{P_CP_D}$. These constrain is not hard to achieve because the length of white dotted line and the interval between the white lines are always same for a normalized road. Obviously, there are many different ways to pick these four points group. Figure 2 shows one general condition. The lane width is a fixed value, so P_A, P_B, P_C, P_D are able to constitute a parallelogram.

In this step, all the corners detected are in the dotted lines, so that the line length as well as lane gap are fixed and the same for the left and right line. By knowing the corner type such as upper-right, down-right, up-left, down-left in a white line, we just need to pick the corner points that make the distance of two points equal. To specify the type of corner, just make simple model match method.

For example, the distance in three consecutive points is always the same. So we can choose $\overline{P_1P_3}$, $\overline{P_2P_4}$, $\overline{P_3P_5}$ in the left and $\overline{P'_1P'_3}$, $\overline{P'_2P'_4}$, $\overline{P'_3P'_5}$ in the right. And the distance between two points belonging to a white line is always the same, so that we can choose $\overline{P_1P_2}$, $\overline{P_3P_4}$ in the left and $\overline{P'_1P'_2}$, $\overline{P'_3P'_4}$ in the right. (Figure 3)

Besides, there are many types of combinations for corner point choosing. Due to many experiments, it is found that when more points in the near range is selected and the distance of $\overline{V_1V_2}$ (see Figure 3) are between $0.5w$ and $1.5w$

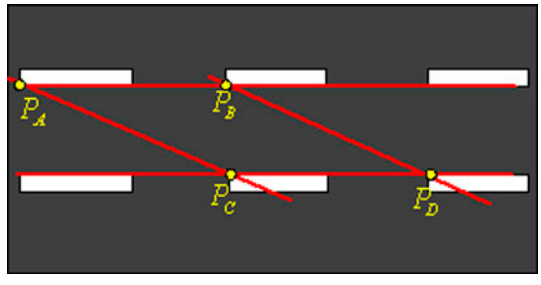

Figure 2. Dotted road line with edge points.

Figure 3. Edge points selection sample.

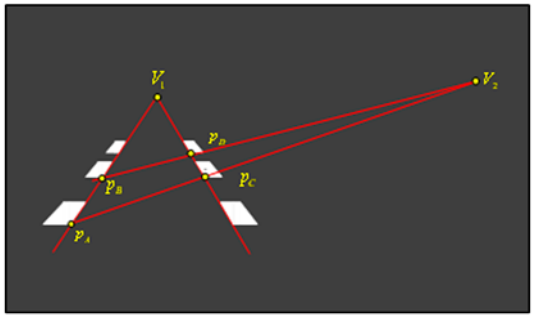

Figure 4. Dotted road line in image.

(w are the image width, $w = 640$ in most cases), the calibration results are the best.

(c) *External parameters deduction*

Based on the projective geometry characteristic of camera pinhole model, any two infinity parallel line in world coordinate system will intersect and terminate at one point in pixel coordinate system. This point is called Vanishing Point. So the situation in Figure 2 in world coordinate is demonstrated in pixel coordinate showed in Figure 4.

According to the analysis above, line $\overrightarrow{p_Ap_B}$, $\overrightarrow{p_Cp_D}$ and line $\overrightarrow{p_Ap_C}$, $\overrightarrow{p_Bp_D}$ will intersect in vanishing points V_1, V_2, respectively. Let the coordinate of p_A, p_B, p_C, p_D and p_A, p_B, p_C, p_D as:

$P_A = [\ x_A \quad y_A \quad z_A\ ]^T$, $P_B = [\ x_B \quad y_B \quad z_B\ ]^T$, $P_C = [\ x_C \quad y_C \quad z_C\ ]^T$, $P_D = [\ x_D \quad y_D \quad z_D\ ]^T$ and $P_A = [\ u_A \quad v_A\ ]^T$, $P_B = [\ u_B \quad v_B\ ]^T$, $P_C = [\ u_C \quad v_C\ ]^T$, $P_D = [\ u_D \quad v_D\ ]^T$.

Linear equation of $\overrightarrow{p_Ap_B}$, $\overrightarrow{p_Cp_D}$ and line $\overrightarrow{p_Ap_C}$, $\overrightarrow{p_Bp_D}$ in the image plane are:

$$\overrightarrow{p_Ap_B}: \frac{x-u_A}{u_A-u_B} = \frac{y-v_A}{v_A-v_B} \tag{6}$$

$$\overrightarrow{p_Cp_D}: \frac{x-u_C}{u_C-u_D} = \frac{y-v_C}{v_C-v_D} \tag{7}$$

$$\overrightarrow{p_Ap_C}: \frac{x-u_A}{u_A-u_C} = \frac{y-v_A}{v_A-v_C} \tag{8}$$

$$\overrightarrow{p_Bp_D}: \frac{x-u_B}{u_B-u_D} = \frac{y-v_B}{v_B-v_D} \tag{9}$$

Since the value of p_A, p_B, p_C and p_D can be got directly from the image, the coordinates of the vanishing points in image are easy to get by calculating:

$$u_{V1} = (u_B-u_A)(v_{V1}-v_A)/(v_B-v_A)+u_A \tag{10}$$

$$v_{V1} = \left(\frac{v_Cu_D-u_Cv_D}{v_C-v_D} - \frac{v_Au_B-u_Av_B}{v_A-v_B}\right)/\left(\frac{u_A-u_B}{v_A-v_B} - \frac{u_C-u_D}{v_C-v_D}\right) \tag{11}$$

$$u_{V2} = (u_C-u_A)(v_{V2}-v_A)/(v_C-v_A)+u_A \tag{12}$$

$$v_{V2} = \left(\frac{v_Bu_D-u_Bv_D}{v_B-v_D} - \frac{v_Au_C-u_Av_C}{v_A-v_C}\right)/\left(\frac{u_A-u_C}{v_A-v_C} - \frac{u_B-u_D}{v_B-v_D}\right) \tag{13}$$

The point P_1 of line $\overrightarrow{p_Ap_B}$ in road plane can be written as $P_1 = [d_1 \quad 0 \quad S]^T$. Based on Equation (4), the

coordinate of p_1 which is the relative point in pixel coordinate system of P_1 can be calculated. The value of $p_1 = [\,u_1 \quad v_1\,]^T$ is:

$$\begin{cases} u_1 = \dfrac{d_1(\alpha_x r_{11} + u_0 r_{31}) + s(\alpha_x r_{13} + u_0 r_{33})}{d_1 r_{31} + s r_{33}} \\ v_1 = \dfrac{d_1(\alpha_y r_{21} + v_0 r_{31}) + s(\alpha_y r_{23} + v_0 r_{33}) - h\alpha_y}{d_1 r_{31} + s r_{33}} \end{cases} \tag{14}$$

The point P_2 of line $\overrightarrow{p_A p_C}$ in road plane also can be written as $P_2 = [\,d_2 \quad 0 \quad a d_2 + b\,]^T$. Also based on Equation (4), the coordinate of p_2 which is the relative point in pixel coordinate system of P_2 can be calculated. The value of $p_2 = [\,u_2 \quad v_2\,]^T$ is:

$$\begin{cases} u_2 = \dfrac{d_2(\alpha_x r_{11} + u_0 r_{31}) + (a d_2 + b)(\alpha_x r_{13} + u_0 r_{33})}{d_2 r_{31} + (a d_2 + b) r_{33}} \\ v_2 = \dfrac{d_2(\alpha_y r_{21} + v_0 r_{31}) + (a d_2 + b)(\alpha_y r_{23} + v_0 r_{33}) - h\alpha_y}{d_2 r_{31} + (a d_2 + b) r_{33}} \end{cases} \tag{15}$$

The vanishing point in image is the infinity point of world coordinate system mapped on the image. To get the theoretical value of vanishing points, just make $s = +\infty$ in Equation (14). The theoretical value of vanishing point $\widetilde{p_1} = [\,\widetilde{u_1} \quad \widetilde{v_1}\,]^T$ is:

Also the same process, make $d_2 = +\infty$, the value of another vanishing point $\widetilde{p_2} = [\,\widetilde{u_2} \quad \widetilde{v_2}\,]^T$ is:

$$\begin{cases} \widetilde{u_1} = \lim\limits_{s \to +\infty} u_1 = u_0 + \dfrac{\alpha_x r_{13}}{r_{33}} = u_0 + \dfrac{\alpha_x \sin\theta \cos\varphi}{\cos\theta \cos\varphi} \\ \qquad\qquad = u_0 + \alpha_x \tan\theta \\ \widetilde{v_1} = \lim\limits_{s \to +\infty} v_1 = v_0 + \dfrac{\alpha_y r_{23}}{r_{33}} = v_0 + \dfrac{-\alpha_y \sin\varphi}{\cos\theta \cos\varphi} \\ \qquad\qquad = v_0 - \alpha_y \tan\varphi / \cos\theta \end{cases} \tag{16}$$

$$\begin{cases} \widetilde{u_2} = \lim\limits_{d_2 \to +\infty} u_2 = u_0 + \frac{\alpha_x r_{11} + a\alpha_x r_{13}}{r_{31} + a r_{33}} \\ = u_0 + \dfrac{\alpha_x(\cos\theta\cos\psi + \sin\theta\sin\varphi\sin\psi) + a\alpha_x \sin\theta\cos\varphi}{-\sin\theta\cos\varphi + \cos\theta\sin\varphi\sin\psi + a\cos\theta\cos\varphi} \\ \widetilde{v_2} = \lim\limits_{d_2 \to +\infty} v_2 = v_0 + \dfrac{\alpha_y r_{21} + a\alpha_y r_{23}}{r_{31} + a r_{33}} \\ = v_0 + \dfrac{\alpha_y \cos\varphi \sin\psi - a\alpha_y \sin\varphi}{-\sin\theta\cos\varphi + \cos\theta\sin\varphi\sin\psi + a\cos\theta\cos\varphi} \end{cases} \tag{17}$$

Since real value and theoretical value of vanishing points are the same, the equation group maintain four equations is established.

$$\begin{cases} u_{V1} = \widetilde{u_1} \\ v_{V1} = \widetilde{v_1} \\ u_{V2} = \widetilde{u_2} \\ v_{V2} = \widetilde{v_2} \end{cases} \tag{18}$$

By observation, it is found that equations just maintain four unknown parameters θ, φ, ψ, and a. So they can be calculated in numerical methods, which means, the external parameters of camera can be obtained.

4. Experiment results

The experiment is constituted with two parts: static experiment and dynamic experiment. The former is to demonstrate the calibration accuracy compared with traditional DLT method. And the latter one is to evaluate the accuracy indirectly with measuring the distance between vehicle in front and ego vehicle.

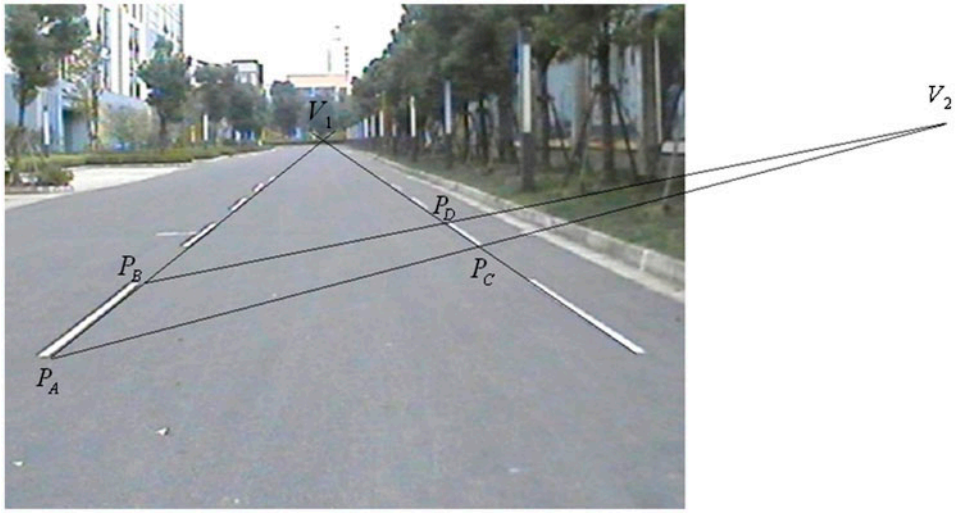

Figure 5. Double parallel lines with vanishing point.

4.1. Static calibration experiment

In the static experiment, a flat road surface around our institute is selected. Then the normalized dotted road lane is drawn artificially. After that the camera is placed between two road lanes.

One image captured from the camera is shown in Figure 5. Using the Calibration method proposed in Section 3, the coordinate of two vanishing points can be measured which are $u_{V1} = 299$, $u_{V1} = 129$ and $u_{V2} = 889$, $u_{V2} = 112$. Besides, the height of camera is known that is $h = 1.35$ m. By solving Equation (8), the three Euler angle is able to get $\theta = -0.0438, \varphi = 0.0737, \psi = -0.0214$, which are the external parameters.

To evaluate this method, another external parameters need to be calculated with DLT method. The lane corner points whose coordinate are known, so it is easy to calculate the external parameters by DLT method. Figure 6 shows those corner points used in DLT method.

Figure 6. Lane edge points for DLT algorithm.

Three typical camera pose are tested. Three images captured in three poses are shown in Figure 7. Figure 7(a–c) simulate the situation that the vehicle go slight left, go middle, and go slight right on the road. The error is definite below:

Let $H_{DLT} = [\,h^1_{dlt} \quad h^2_{dlt} \quad h^3_{dlt}\,]^T$ and $H_{DRL} = [\,h^1_{drl} \quad h^2_{drl} \quad h^3_{drl}\,]^T$ stand for the external matrix calcu-

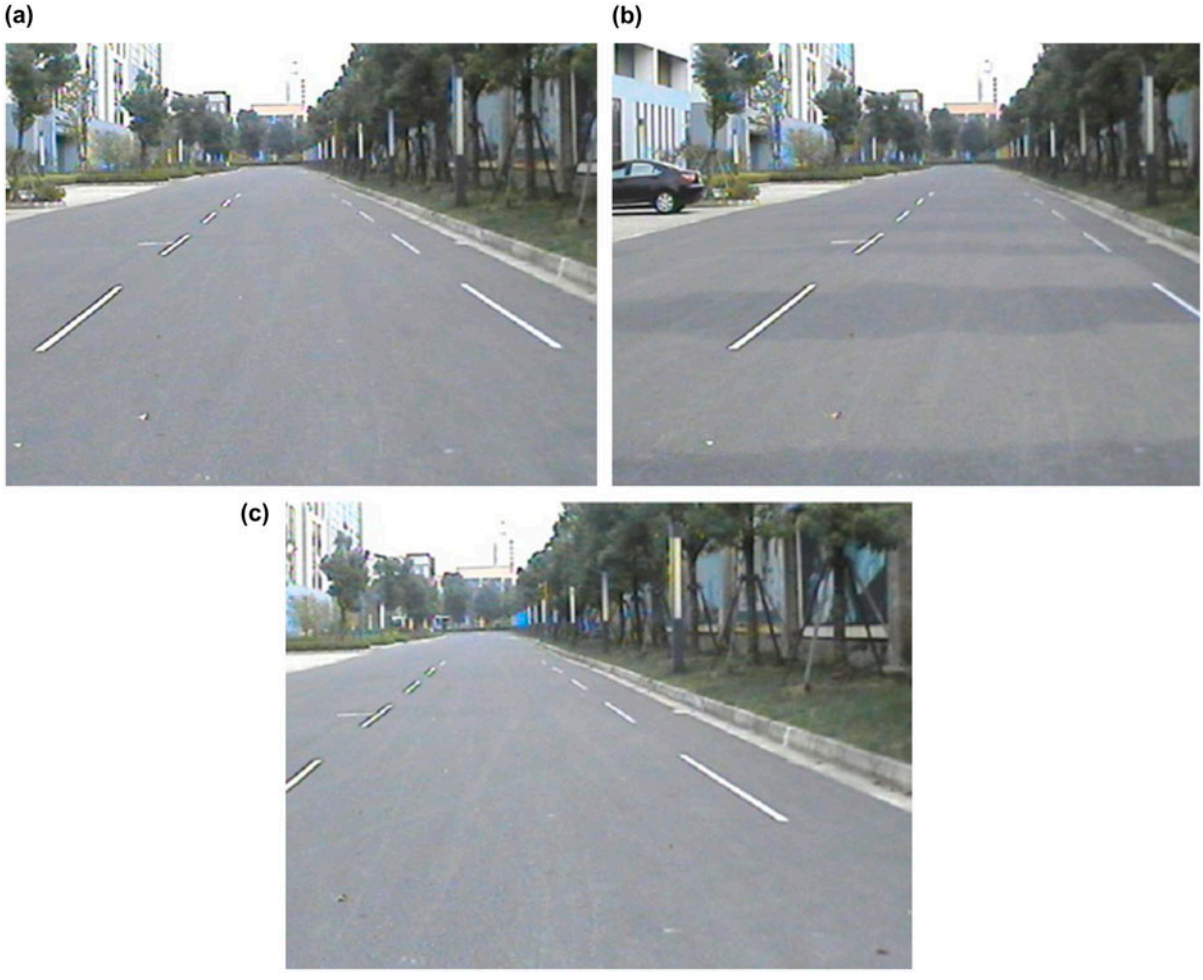

Figure 7. Road image captured in different camera pose.

lated with DLT method and our DRL (dashed road lane based) method. The error metric is calculated below, $L_2(*)$ means two norm of a vector:

$$\text{Error} = \frac{L_2(L_2(h^1_{dlt} - h^1_{drl}), L_2(h^2_{dlt} - h^2_{drl}), L_2(h^3_{dlt} - h^3_{drl}))}{L_2(L_2(h^1_{dlt}), L_2(h^2_{dlt}), L_2(h^3_{dlt}))} \tag{19}$$

Table 1 demonstrates the compare results of our method and DLT method. It can be seen from the table that the error between these two methods is less than 3%.

4.2. Dynamic calibration experiment

In the dynamic test, because it is difficult to obtain camera external parameters in real time by other methods, we adopt an indirect comparison way for evaluation.

Specific methods are as follows: writing a GUI program. Experimenter can manually select the down side of the vehicle in front. Then using the real-time updated camera parameters of our method, the distance s_Camera between the vehicle in front and ego vehicle can be obtained. Meanwhile, the ego vehicle equip with a laser which can access the distance s_Laser of the front vehicle. By comparison of these two distances, it can partially demonstrate the accuracy of the algorithm (Figure 8).

An experiment is taken in Shanghai–Nanjing Freeway (G42 Freeway) (Table 2) at daytime. From the results it can be seen that the average error is around about 3.3%. In analysis, it can be seen that the error is partly caused by camera parameter calibration error and partly caused due to the discrete of image pixels. When the distance is big, the latter factor takes greater proportion. Therefore, near range distance error is more close to the calibration algorithm error which is less than 3%.

4.3. Further analysis

Obviously, the accuracy of the proposed algorithm will be affected by many factors among which corner extraction accuracy and lane normalization degree are the

Table 2. Comparative results of distance got with two sources.

	s_Camera (m)	s_Laser (m)	Error (%)
8(a)	139.3	147	5.24
8(b)	128.6	134	4.03
8(c)	108.8	112	2.86
8(d)	98.4	101	2.57
8(e)	70.1	72	2.64
8(f)	57.6	59	2.37

Table 1. Camera external parameters with two methods.

	Our method H_{DRL}	DLT method H_{DLT}	Error (%)
7(a)	$\begin{bmatrix} 0.9990 & -0.0028 & -0.0437 \\ -0.0004 & 0.9973 & -0.0736 \\ 0.0436 & 0.0736 & 0.9963 \end{bmatrix}$	$\begin{bmatrix} 0.9992 & -0.0028 & -0.0406 \\ -0.0005 & 0.9966 & -0.0825 \\ 0.0406 & 0.0824 & 0.9958 \end{bmatrix}$	0.99
7(b)	$\begin{bmatrix} 0.9897 & -0.0107 & -0.1428 \\ -0.0009 & 0.9967 & -0.0810 \\ 0.1428 & 0.0803 & 0.9864 \end{bmatrix}$	$\begin{bmatrix} 0.9925 & -0.0101 & -0.1220 \\ -0.0010 & 0.9959 & -0.0907 \\ 0.1219 & 0.0902 & 0.9884 \end{bmatrix}$	2.52
7(c)	$\begin{bmatrix} 0.9923 & 0.0064 & 0.1239 \\ 0.0012 & 0.9981 & -0.0611 \\ -0.1239 & 0.0607 & 0.9904 \end{bmatrix}$	$\begin{bmatrix} 0.9894 & 0.0082 & 0.1447 \\ 0.0014 & 0.9978 & -0.0659 \\ -0.1446 & 0.0654 & 0.9873 \end{bmatrix}$	2.44

Figure 8. Image sequence for distance measurement.

greatest impacts. In this section, the effects of these two factors will be analyzed by further experiments.

4.3.1. Analysis of corner extraction and calibration accuracy

With the dynamic experiment method in Section 4.2, more than 10 experiments in different time are actuated. The average corner extraction error and average distance measure error are recorded. It demonstrates that the average error is around 1.7 pixel-distances in captured 640 × 480 image. The data of five typical scenarios are shown in Table 3 from which it can be seen that with the increase of corner extraction error, the calibration error increase subsequently.

It should be mentioned that, when the experiment is taken in the dark night. Due to the extremely bad illumination, the corner detection algorithm is failed so that the calibration process ended.

4.3.2. Analysis of calibration accuracy in lane with different interval

Although the interval between road lanes is same under ideal conditions, in actual road environment, the interval might have slight variance. To evaluate the stability of the algorithm in this situation, some extra experiments are made.

These experiments are partly similar to that made in Section 4.1 in which the dotted road lane is drawn artificially. What is the difference is that the interval between dotted road lanes is not always the same. As shown in Figure 9, the lane interval is equal in Figure 9(a) while the lane interval of one group of lanes is intentionally changed with 5 cm (Figure 9(b)). In this situation, the calibration results are shown in Table 4. It can be seen

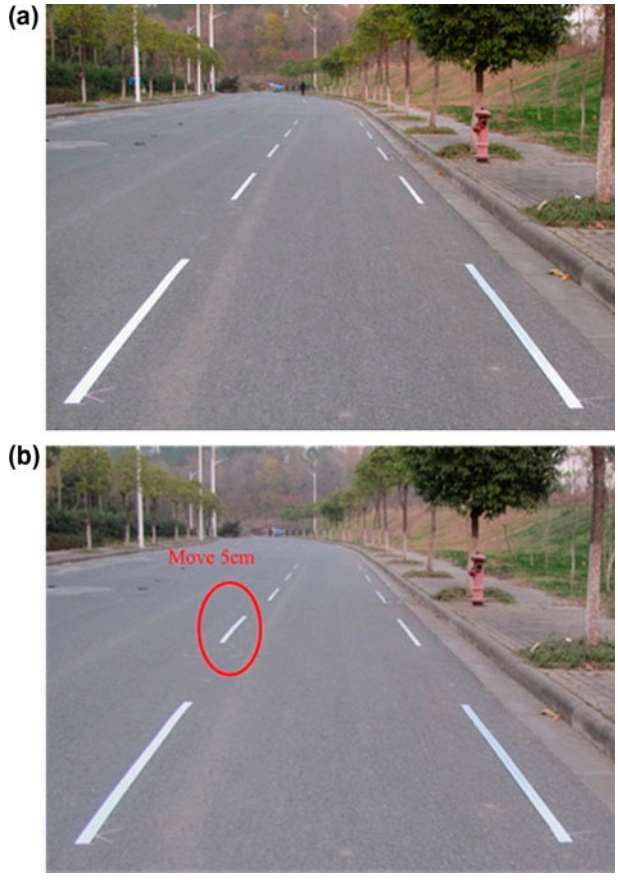

Figure 9. Road image with different lane interval.

Table 3. Corner error and distance measure error.

Experiment no.	Scenario description	Corner extraction error	Distance measure error (%)
1	Freeway_morning1	1.81	4.0
2	Freeway_morning2	1.44	3.4
3	Freeway_noon1	1.11	2.6
4	Freeway_afternoon1	1.66	3.7
5	Freeway_afternoon2	2.16	4.9

Table 4. Camera external parameters with lane interval change.

	Our method H_{DRL}	DLT method H_{DLT}	Error (%)
9(a)	$\begin{bmatrix} 0.9992 & -0.0073 & -0.0400 \\ -0.0005 & 0.9811 & -0.1933 \\ -0.0399 & 0.1932 & 0.9803 \end{bmatrix}$	$\begin{bmatrix} 0.9990 & -0.0072 & -0.0431 \\ -0.0004 & 0.9850 & -0.1728 \\ 0.0431 & 0.1727 & 0.9840 \end{bmatrix}$	2.11
9(b)	$\begin{bmatrix} 0.9995 & -0.0056 & -0.0302 \\ -0.0006 & 0.9791 & -0.2035 \\ 0.0300 & 0.2035 & 0.9786 \end{bmatrix}$	$\begin{bmatrix} 0.9990 & -0.0072 & -0.0431 \\ -0.0004 & 0.9850 & -0.1728 \\ 0.0431 & 0.1727 & 0.9840 \end{bmatrix}$	3.39

that, the calibration error rise from 2.11 to 3.39% in this situation. It should be mentioned that we also move the lane to 10 and 15 cm separately; the error rises to 5.71 and 10.10% each.

5. Conclusion

In practical application of automotive vision systems, the on-board camera's external parameters may change as the vehicle is moving. To solve this problem, it is found that dotted lane corner connections can constitute two sets of parallel lines. Through theoretical derivation, an online camera's external parameters calibration method is proposed which can be acted without any human intervention. Experiment results and comparison show that the method is simple, maintain relatively high accuracy, and can meet typical active safety application like lane departure warning, collision warning.

To use this method, two straight dotted road lanes is necessary. Our next job is to figure out whether it is possible to get the external parameters with two curved dotted road lane or just one dotted road lane.

Acknowledgements

This research was funded partly by the National Key Technology R&D Program of China during the 11th Five-Year Plan Period (2009BAG13A04), Jiangsu Province Colleges and Universities Natural Science Foundation (13KJD520003) and partly by Jiangsu University Scientific Research Foundation for Senior Professionals (12JDG10).

Notes on contributors

Hai Wang was born in Zhenjiang City, China in 1983. He received the BS degree in Measure and Control Technology in 2006 and the PhD degree in Instrument Science and Technology in 2012 from the School of Instrument Science and Engineering, Southeast University, Nanjing, China. He is currently an assistant professor in School of Automotive and Traffic Engineering, Jiangsu University, Zhenjiang, China. His research interests include computer vision, machine learning, intelligent vehicles, and transportation systems.

Yingfeng Cai was born in Nantong City, China in 1985. She received the BS degree in Measure and Control Technology in 2006, the MS degree in Precision Instrument and Machinery in 2009 and PhD degree in Instrument Science and Technology in 2013 from the School of Instrument Science and Engineering, Southeast University, Nanjing, China. She is currently an assistant professor in School of Automotive and Traffic Engineering, Jiangsu University, Zhenjiang, China. Her research interests include computer vision, machine learning, intelligent vehicles, and transportation systems.

Guoyu Lin was born in Fuzhou City, China in 1979. He received the BS degree in measure and control technology in 2002, the MS degree in precision instrument and machinery in 2005 and PhD degree in Instrument Science and Technology in 2008 from the School of Instrument Science and Engineering, Southeast University, Nanjing, China. He is currently an associate professor with the School of Instrument Science and Engineering, Southeast University. His research interests include computer vision, intelligent vehicles, transportation systems, and advanced automobile testing technology.

Weigong Zhang received the MS degree in Solid Mechanics from Nanjing University of Aeronautics and Astronautics, Nanjing, China, in 1986 and the PhD degree in Instrument Science and Technology from the Southeast University, Nanjing, in 2001. He is currently a professor with the School of Instrument Science and Engineering, Southeast University. His research interests include intelligent vehicles, advanced automobile testing technology, and advanced vehicle navigation & control.

References

[1] Schoepflin T, Dailey D. Dynamic camera calibration of roadside traffic management cameras for vehicle speed estimation. IEEE Trans. Intell. Transp. Syst. 2003;4:90–98.
[2] Mirzaei F, Roumeliotis S. A Kalman filter-based algorithm for IMU-camera calibration: observability analysis and performance evaluation. IEEE Trans. Rob. 2008;24:1143–1156.
[3] Gehrig S, Stein F. Collision avoidance for vehicle-following systems. IEEE Trans. Intell. Transp. Syst. 2007;8:233–244.
[4] Giseok K, Jae-soo C. Vision-based vehicle detection and inter-vehicle distance estimation. 12th International Conference on Control, Automation and System. 2012;625–629.
[5] Lili H. Roadside camera calibration and its application in length-based vehicle classification. 2nd International Asia Conference on Informatics in Control, Automation and Robotics (CAR). 2010;j.2:329–332.
[6] Wender S, Dietmayer K. 3D vehicle detection using a laser scanner and a video camera. IET Intell. Transport Syst. 2008;2:105–112.
[7] Miyagawa I, Arai H, Koike H. Simple camera calibration from a single image using five points on two orthogonal 1-D objects. IEEE Trans. Image Process. 2010;19:1528–1538.
[8] Jing H, Yang B, Yuhao Y. A method of vehicle camera self-calibration. 2010 3rd International Congress on Image and Signal Processing (CISP). 2010;j.5:2449–2453.

[9] Miksch M, Yang B, Zimmermann K. Automatic extrinsic camera self-calibration based on homography and epipolar geometry. 2010 IEEE Intelligent Vehicles Symposium. 2010;j.1:832–839.
[10] Wu M, An X. An automatic extrinsic parameter calibration method for camera-on-vehicle on structured road. IEEE Int. Conf. Veh. Electron. Saf. 2007;j.3:1–5.
[11] Li Q, Zheng N, Zhang X. Calibration of external parameters of vehicle-mounted camera with trilinear method. Opto-Electron. Eng. 2004;j.31:23–26.
[12] Yu H, Zhang W. Lane departure detection for moving vehicle based on camera model. J. Southeast Univ. (Natural Science Edition). 2009;J.39:933–936.
[13] Chen Q, Wang H. A real-time lane detection algorithm based on a hyperbola-pair model. Intelligent Vehicles Symposium 2006; 2006 June 13–15; Tokyo, Japan